

## First Lunar Occultation Results with the TIRCAM2 Near-Infrared Imager at the Devasthal 3.6-m Telescope

Saurabh Sharma<sup>1,4</sup>, Andrea Richichi<sup>2</sup>, Devendra K. Ojha<sup>3</sup>, Brajesh Kumar<sup>1</sup>, Milind Naik<sup>3</sup>,  
Jeewan Rawat<sup>1</sup>, Darshan S. Bora<sup>1</sup>, Kuldeep Belwal<sup>1</sup>, Prakash Dhama<sup>1</sup> and Mohit Bisht<sup>1</sup>

<sup>1</sup>Aryabhata Research Institute of Observational Sciences  
Manora Peak, Nainital 263002, India

<sup>2</sup>INAF — Osservatorio Astrofisico di Arcetri  
Largo E. Fermi 5, I-50125 Firenze, Italy

<sup>3</sup>Tata Institute of Fundamental Research  
Homi Bhabha Road, Colaba, Mumbai 400005, India

<sup>4</sup>saurabh@aries.res.in

Received June 30, 2022; Revised September 14, 2022; Accepted November 3, 2022; Published February 23, 2023

TIRCAM2 is the facility near-infrared Imager at the Devasthal 3.6-m telescope in northern India, equipped with an Aladdin III InSb array detector. We have pioneered the use of TIRCAM2 for very fast photometry, with the aim of recording Lunar Occultations (LO). This mode is now operational and publicly offered. In this paper, we describe the relevant instrumental details, provide references to the LO method and the underlying data analysis procedures, and list the LO events recorded so far. Among the results, we highlight a few which have led to the measurement of one small-separation binary star and of two stellar angular diameters. We conclude with a brief outlook on further possible instrumental developments and an estimate of the scientific return. In particular, we find that the LO technique can detect sources down to  $K \approx 9$  mag with  $\text{SNR} = 1$  on the Devasthal Optical Telescope telescope. Angular diameters larger than  $\approx 1$  milli-arcsecond (mas) could be measured with  $\text{SNR}$  above 10, or  $K \approx 6$  mag. These numbers are only an indication and will depend strongly on observing conditions such as lunar phase and rate of lunar limb motion. Based on statistics alone, there are several thousands LO events observable in principle with the given telescope and instrument every year.

*Keywords:* Instrumentation; detectors; methods; observational; occultations; stars: individual.

### 1. Introduction

Recently, the 3.6-m Devasthal Optical Telescope (DOT) started operations as the largest facility of its kind in India (Kumar *et al.*, 2018). It is located at 2450 m elevation, longitude of 79.7E, latitude of 29.4N, and managed by the Aryabhata Research Institute of Observational Sciences (ARIES; Nainital). The telescope has a 3.6-m active-control primary mirror, Ritchey–Chretien optics, an alt-azimuth mount and a corrected science field of view (FoV) of 30' at the Cassegrain focus. It is equipped with various Imager and spectrographs operating from the visual to the near-infrared (NIR) range

(Baug *et al.*, 2018; Ojha *et al.*, 2018; Omar *et al.*, 2019; Kumar *et al.*, 2022). The site is operated for eight months which are not affected by the monsoon rainfall, i.e. October–May, in two observational cycles. The median seeing at Devasthal is around 1''1 (at ground level in optical bands), although best values can approach 0''6 at the 3.6-m DOT height (Stalin *et al.*, 2001).

In this paper, we focus on the instrumental requirements and scientific aspects relative to the observation of Lunar Occultation (LO) events at DOT in the NIR. The LO technique consists in recording and analyzing the diffraction pattern generated when the lunar limb moves over a background source, and it is especially attractive

<sup>4</sup>Corresponding author.

since it achieves angular resolution far exceeding the diffraction limit of the telescope. Given the typical angular rate of the limb, it generally requires time resolutions of few ms. A strong tradition already started in India at the 1.2-m Mount Abu telescope three decades ago (Chandrasekhar et al., 1993) with a single-pixel InSb detector and later continued with a NIR focal plane array (FPA) detector (e.g. Chandrasekhar & Baug, 2010). More recently, observations have continued at ARIES using a frame transfer Andor iXon EMCCD on the 1.3-m telescope also located at Devasthal (e.g. Richichi et al., 2017, 2020). This is however the first time that a considerably larger telescope is employed for fast photometric observations in India. A mention of two initial LO events recorded with the TIRCAM2 (TIFR Near Infrared Imaging Camera-II, the only instrument on 3.6 m DOT which is capable in doing millisecond sampling) instrument at the 3.6-m DOT was given in Richichi et al. (2020). In this paper, we provide full details of this operational mode in Sec. 2, and present the complete commissioning results. We will briefly describe the method and the associated data analysis in Sec. 3. A total of 12 LO events have been successfully recorded at DOT using TIRCAM2 to date, of which one has led to the measurement of two binary stars and two resolved stellar diameter. We will discuss these results in Sec. 4, while in Sec. 5, we will outline how we intend to further improve the instrumental aspects in order to achieve higher temporal resolution, and the scientific strategy for this specialized mode of observation at DOT.

## 2. TIRCAM2 and Its Adaptation for Fast Photometry

TIRCAM2 is a closed-cycle cooled Imager that has been developed by the Infrared Astronomy Group at Tata Institute of Fundamental Research for observations in the NIR range (Naik et al., 2012). TIRCAM2 is sensitive between  $1\ \mu\text{m}$  and  $5\ \mu\text{m}$  and includes both the standard NIR broad-band filters  $J$ ,  $H$ ,  $K$ , as well as several narrow-band filters, namely  $K_{\text{cont}}$ , Brackett–Gamma, Polycyclic Aromatic Hydrocarbon (PAH) and  $L$ -narrow. TIRCAM2 uses a  $512 \times 512$  InSb Aladdin III Quadrant FPA, which corresponds to  $86''5 \times 86''5$  FoV on 3.6 m DOT with a plate scale of  $0''169/\text{pixel}$ . It is

cooled to an operating temperature of 35 K by a closed cycle Helium cryo-cooler. A schematic picture of TIRCAM2 showing its different components is presented in Fig. 1. More details on TIRCAM2 can be found in Ghosh et al. (2022) and Baug et al. (2018). TIRCAM2 is currently the only NIR imaging camera in India which can observe up to  $L$  band in the NIR. Therefore, this camera could be a good complementary instrument to observe the bright nbL-band sources that are saturated in the Spitzer-Infrared Array Camera (IRAC) Ch1-band ( $[3.6] \cdot 7.92$  mag) and the WISE W1-band ( $[3.4] \cdot 8.1$  mag). Sources with strong PAH emission at  $3.3\ \mu\text{m}$  are also observable with TIRCAM2 (Baug et al., 2018). In our initial LO commissioning observations reported here, we have used only the broad-band  $K$  filter but any of the other available filters could be used too, depending on the trade-off between sensitivity and sky background for the given science case. The dark current measured is  $\approx 12\ \text{e}^-/\text{s}$  and the readout noise  $\approx 30\ \text{e}^-$ . The median gain of the detector is  $\approx 10\ \text{e}^-/\text{ADU}$ .

Due to the elevated sky background in the NIR, typical exposure times per frame with TIRCAM2 for conventional imaging are already considerably shorter than for visual range instrumentation and of order  $\approx 10$  s. In fact, individual exposures of the full FPA can be captured in as short as 256 ms. However, this is far too slow for our LO application which requires individual exposures in the ms range. Thus, we developed a fast photometry mode, in which the data are captured in  $32 \times 32$  pixels sub-array, corresponding to about  $5''4 \times 5''4$  on the sky. As the full width at half-maximum of the stellar images at the 3.6-m DOT is typically  $\sim 0''7$  in the NIR, this is sufficient for photometry including a reasonable sampling of the surrounding sky background. The sub-array is positioned around the target by providing its  $x$  &  $y$  FPA coordinates to the TIRCAM2 software.

The read-out software of TIRCAM2 comprises three individual programs residing in the computer, in the PCI board Digital Signal Processor (DSP), and in the controller DSP, respectively. To achieve a faster readout, the sub-array mode required modifications in both the computer JAVA code and the controller DSP assembly code. With the current version of the software, the sampling time is  $\sim 10$  ms for sub-array mode of TIRCAM2. After the

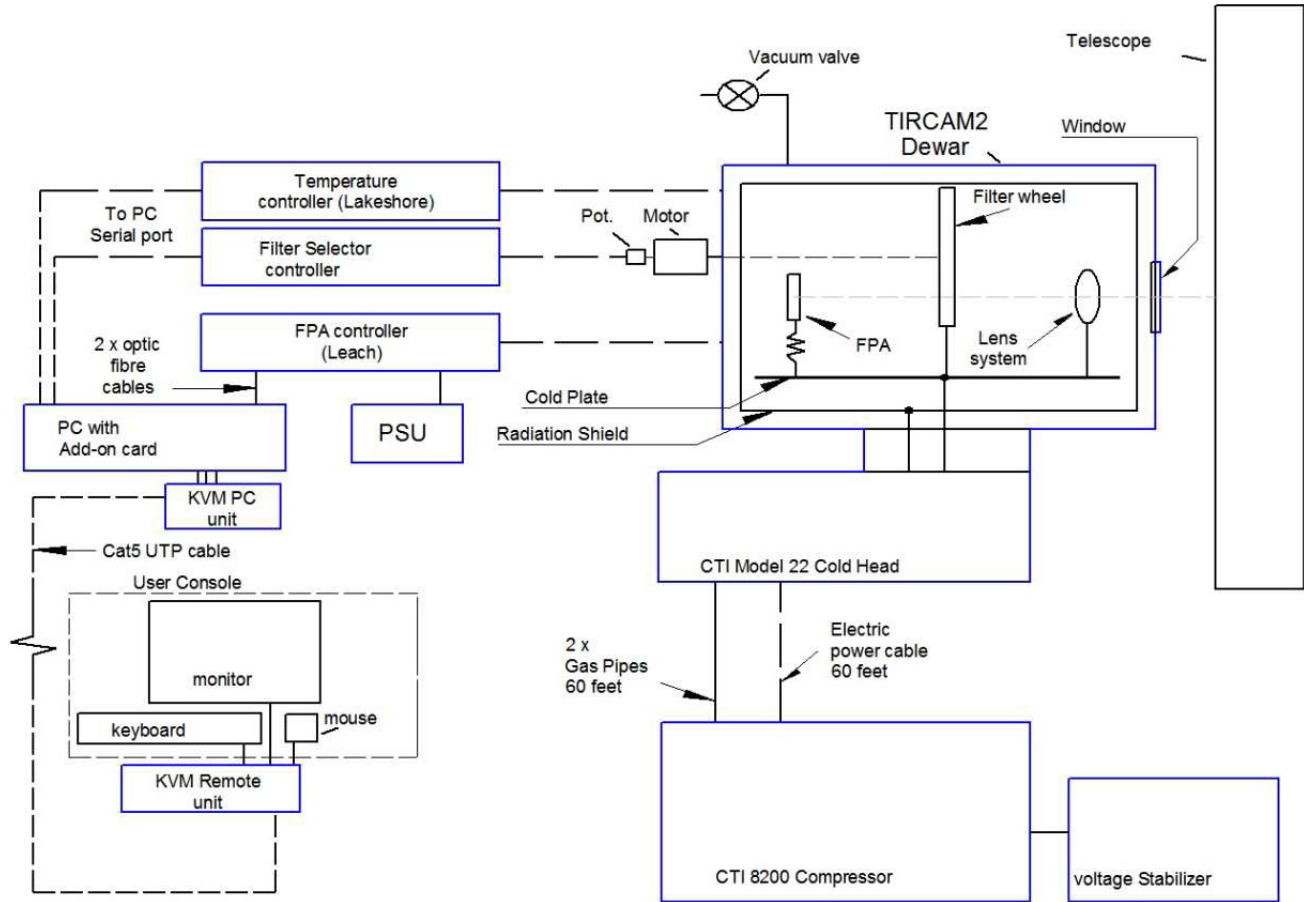


Fig. 1. A schematic picture showing different components of TIRCAM2 which are mounted on the telescope (Dewar, Temperature/Filter/FPA controllers, cold head, PC, etc.), located on the telescope floor (compressor, voltage stabilizer) and located at the observing floor (remote access PC).

sub-array is programmed and initialized in the controller, it captures the required frames and the data are stored in a single FITS file on the computer. In case of the capture box ( $32 \times 32$  pixels) being at the center of FPA, after the FPA is reset, it integrates light for  $\sim 1.7$  ms until capture box digitization is started. Digitization continues for another  $\sim 3.2$  ms and then it continues skipping the remaining rows for another  $\sim 1.7$  ms. The dead time between each frame is around 3.2 ms. So, the total exposure time for the capture box is  $\sim 4.9$  ms and the total time between the consecutive frames is  $\sim 9.8$  ms. As it takes  $\sim 0.007$  ms to skip a row of FPA, the exposure time depends on where the star is located on FPA and can range from 3.2 ms to 6.6 ms. It is possible to reduce the integration time by placing the capture box close to the start row of the FPA. This was not done for the present commissioning work. For LO observation, we generally take 4000 frames requiring  $\sim 40$  s detector illumination, and about 2 min in total including overheads.

### 3. The Lunar Occultation Technique

LO represented the method of choice to achieve milliarcsecond (mas) resolution mainly in the 1970–1990’s. We mention briefly that the technique consists in recording the Fresnel diffraction pattern generated when the lunar limb moves over a distant background source. The limb rate is typically  $\approx 0.7$  m/ms, the event lasts a small fraction of a second, and detection rates of few ms are required to adequately sample the fringes. The principles of data reduction were first formulated by [Nather & McCants \(1970\)](#), while more details and advanced procedures can be found in [Richichi \*et al.\* \(1996\)](#).

Albeit significantly limited in the choice of targets by the orbit of the Moon and by being fixed-time events, LO offer several advantages including a very efficient use of telescope time, a fast and simple data reduction coupled with the ability to derive model-independent results, and an angular

resolution which is rather independent of seeing and telescope diameter.

Recently, more sophisticated methods like long-baseline interferometry and to some extent adaptive-optics and speckle interferometry are now available for similar studies at selected large facilities, but they are typically more time consuming and limited by the need of suitable reference stars. LO still occupy an attractive niche and offer a favorable combination of angular resolution and sensitivity especially at relatively small telescopes where other methods are not an option.

Following a large program of routine LO observations at the ESO VLT in the NIR which yielded over 1000 recorded events about a decade ago with a corresponding large number of new angular diameters and binary stars (Richichi et al., 2014, and references therein), several observatories have now implemented this technique. Examples include the Russian 6-m telescope, and several other facilities such as the 1.3-m telescope also at Devasthal, the 1.2-m and 1.8-m telescopes at Asiago in Italy, the 2.4-m Thai National telescope, the 1.2-m MAO telescope in Trebur, Germany, and the 3.5-m Telescope Nazionale Galileo (TNG) in La Palma, Spain.

LO are essentially a 1D technique, along the direction of the lunar limb motion. Therefore, only the combined observation from different sites offers the opportunity to obtain a 2D view (see e.g. Richichi et al., 2017). Coordinated observations also provide the opportunity for multi-wavelength coverage. In this respect, we stress that TIRCAM2 at DOT is ideally positioned to complement similar observations from East Asia to Europe, and that it is the only facility at present offering NIR coverage.

We remark that while LO observations are possible at any wavelength and there are examples in the literature spanning from ultraviolet to mid-infrared, the NIR range is often considered an ideal range. This is due to the combination of various nonlinear effects: the sky background (mainly scattering of the reflected solar light from the Moon), the thermal background from the lunar surface, the fringe speed decreases with wavelength (which translates to better fringe sampling for a fixed detector cycle), the spectral energy distribution of the occulted source which is often rising towards longer wavelengths for evolved stars and object with dust envelopes.

LO data reduction is considerably less intensive than all other high angular resolution techniques both in terms of data volumes and in required

computing power. It is also unique in the sense of being rather insensitive to seeing conditions and without the need for a reference star. Two different approaches are possible. First, a model-dependent least-square method that includes the estimation of several parameters, including the lunar limb rate which translates to the position angle of the 1D scan, and the angular diameter of the occulted source. It is described e.g. in Richichi et al. (1992), while Richichi et al. (1996) described a method to put an upper limit on the diameter of unresolved sources depending on the noise in the data. With a completely different approach based on an iterative deconvolution technique, Richichi (1989) introduced a method (dubbed composite algorithm) to achieve a model-independent reconstruction of the brightness profile in the maximum-likelihood sense. Examples of the use of these methods are provided in Sec. 4.

#### 4. Commissioning and First Results

We report here the initial commissioning observations of the fast photometric mode of TIRCAM2 at the 3.6-m DOT. They were all carried out using a broad-band  $K$  filter centered at  $2.2\ \mu\text{m}$ . The list of observations is provided in Table 1, where the columns are largely self-explanatory. The predicted time is listed rounded down to the nearest minute, while El and Ill are the Moon's elevation above the horizon and the illuminated fraction. A negative or positive Ill value denotes reappearance or disappearance, respectively. The entries in the next columns are from the SIMBAD database, and SNR is the signal-to-noise ratio for the best possible fit using, depending on the case, models of a point-source, of a resolved stellar diameter, or of a binary star. Some comments are given under Notes, where UR stands for unresolved. We clarify that in case of good SNR, it is possible to put an upper limit on the angular size even if it remains unresolved, as is the case for SAO 77838.

It can be seen that a first run on October 7, 2017 did not produce usable data also given the difficulty of blind pointing due to the events being reappearances, but it allowed us to fine tune the electronics parameters and read-out process. Since the window size of  $32 \times 32$  pixels on 3.6-m DOT corresponds to only  $\sim 5''.4 \times 5''.4$  on sky, the blind pointing is not advised in the case of the re-appearance events (the telescope usually have more  $\sim 2$  arcsec rms pointing errors). What we can do is to calculate the



Table 1. List of LO events observed with TIRCAM2 at DOT.

Source	Date	Time	El	Ill	V	K	Sp	SNR	Notes
TYC639-399-1	7 Oct 17	15 47	25°	−95%	10.8	6.5	M2 III	—	
TYC642-458-1	7 Oct 17	18 15	56°	−94%	10.7	6.8		—	
Mu Cet	7 Oct 17	20 04	71°	−94%	4.1 <sup>a</sup>	3.5	A9IIIp	—	( <sup>1</sup> )
IRC + 20156	18 May 18	14 32	23°	+13%	8.0	2.6		30.4	UR <sup>2</sup>
SAO 98770	21 May 18	20 04	22°	+45%	9.4	7.8	F8	18.1	binary <sup>3</sup> ( $177 \pm 0.4$ mas)
SAO 165154	12 Nov 21	17 27	21°	+63%	9.0	6.2	K1III	—	
BD + 00149	15 Nov 21	20 32	20°	+89%	7.0	4.2	G8III	34.1	UR
IRC + 10032	15 Dec 21	14 42	68°	+90%	7.6	2.6	M	71.9	diameter ( $2.22 \pm 0.25$ mas)
HD 284115	14 Jan 22	12 45	45°	+90%	8.1	4.2	K2	17.8	UR
HD 32380	14 Jan 22	13 17	51°	+90%	8.3	5.2	K0III	—	
103 Tau	14 Jan 22	16 34	83°	+91%	5.5	5.3	B2V	12.55	binary ( $16.8 \pm 0.4$ mas)
IRC + 20101	14 Jan 22	18 57	54°	+91%	8.9	2.7	M0	39.2	diameter ( $2.39 \pm 0.28$ mas)
SAO 77800	15 Jan 22	14 59	63°	+95%	6.6	4.5	K0III	12.9	UR
SAO 77838	15 Jan 22	16 36	83°	+96%	9.1	3.8	K7	66.5	upper limit ( $1.45 \pm 0.65$ mas)
IRC + 30138	15 Jan 22	22 03	26°	+96%	7.6	2.6	M5Ib	—	
IRAS 04269 + 2252	9 Mar 22	14 41	54°	+43%	11.3 <sup>b</sup>	4.7	IR Source	4.0	UR
IRAS 04278 + 2253	9 Mar 22	15 20	46°	+43%	15.0 <sup>a</sup>	5.9	F1, YSO	9.0	UR
IRC + 20084	9 Mar 22	15 59	37°	+43%	7.1	2.9	K5III	16.4	UR

Notes: <sup>1</sup>Observed simultaneously at the 1.3-m telescope.

<sup>2</sup>16 ms sampling.

<sup>3</sup>First near-IR measurement. Discussed in detail in [Richichi et al. \(2020\)](#). 32 ms sampling.

<sup>a,b</sup>R and G magnitudes, respectively.

Events with “—” in the SNR column were not detected, for reasons ranging from sensitivity to pointing issues to timing.

pointing offsets from a pre-identified nearby star and apply those to the target star during the event. The same procedure was adopted while carrying our re-appearances events from the 1.3-m Devasthal Fast Optical Telescope (DFOT) ([Richichi et al., 2020](#)). We also note that some of the events in Table 1 occurred with a very high lunar phase. This resulted in a higher than usual background due to proximity of sunlight reflected off the lunar surface, and more photon noise in the data as a consequence. We expect that under average conditions the SNR for similar magnitudes might be better than reported in Table 1. We emphasize that the few selected results that we discuss in the following are affected by relatively large uncertainties, as is to be expected given the slower than ideal time sampling, and in general by the commissioning nature of the observations. They are mainly intended to verify the feasibility of LO with TIRCAM2, and to encourage future users of this method. We are also striving to improve the SNR performance in the near future, as discussed in Sec. 5.

#### 4.1. IRC + 10032

Our data for IRC + 10032 are shown on the left side of Fig. 2, together with a best fit by a uniform disk

(UD) angular diameter of  $2.22 \pm 0.25$  mas. Interestingly, the first high angular resolution measurement of this M giant was also an LO in the *K*-band reported by [Tej & Chandrasekhar \(2000\)](#), who found it unresolved with an upper limit of 2 mas. Recently, [Robbe-Dubois et al. \(2022\)](#) accurately measured the UD diameter of IRC + 10032 (HD 17973) to be  $1.93 \pm 0.015$  mas in the *L* band. Our measurement is roughly consistent with this value.

#### 4.2. 103 Tau

The data and fit for 103 Tau are shown in Fig. 3, together with a model-independent reconstruction of the brightness profile obtained with the CAL method mention in Sec. 3. The reduced contrast of the main fringe is highly suggestive of the presence of a companion, which is clearly revealed in the model-independent analysis, see Fig. 3. From the binary fit, we find a projected separation of  $16.8 \pm 0.4$  mas along position angle  $PA = 165^\circ$ , and a brightness difference from the primary of  $2.31 \pm 0.04$  mag.

The companion to 103 Tau had already been detected from a number of investigations using speckle interferometry, e.g. among the most recent ones [Horch et al. \(2015\)](#) and [Guerrero et al. \(2020\)](#).

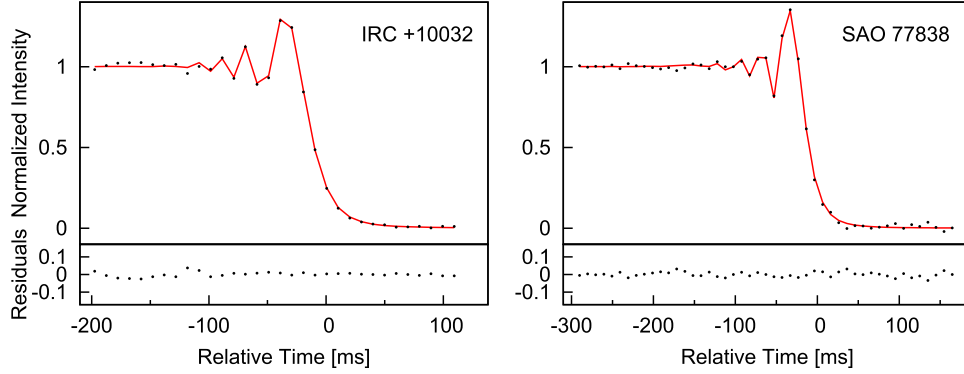


Fig. 2. Left: LO data normalized in intensity for IRC + 10032 (dots) and best fit by a model with a stellar diameter of 2.2 mas (line) are shown in the top panel. Right: the same for SAO 77838, fitted by a point-source model. Note the higher fringe contrast for the unresolved star case. The two bottom panels show the respective fit residuals. Details are given in the text.

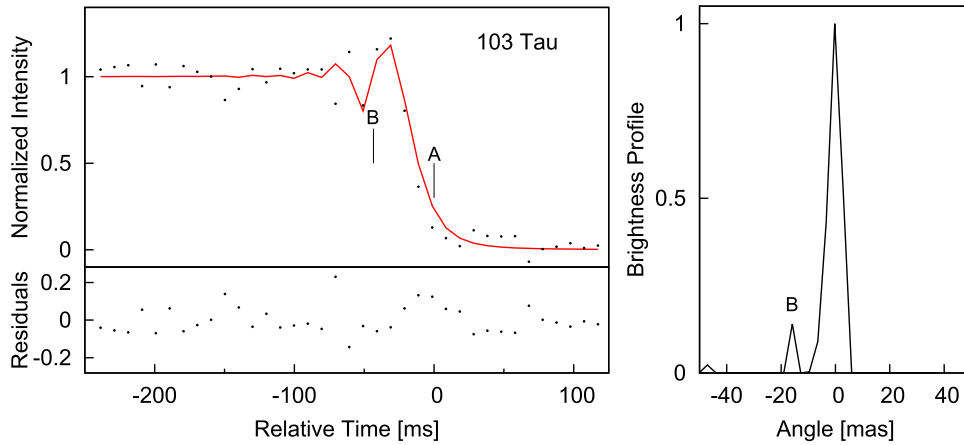


Fig. 3. Left: LO data normalized in intensity for 103 Tau (dots) and best fit by a binary model (line) are shown in the top panel, while the bottom panel shows the fit residuals. The position in time of the components is shown, with the secondary being occulted about 43 ms before the primary. Right: a model-independent brightness profile reconstruction, showing the binary nature of 103 Tau. Details are given in the text.

This is however the first time that it is detected in the NIR, and our flux ratio determination of 1:8.3 ( $\pm 0.3$ ) well agrees with the spectral classification of primary and secondary being both B dwarfs with a few sub-classes difference, see e.g. Tarasov (2016) using spectroscopic investigations.

### 4.3. IRC + 20101

For this source, we find that a fit by a resolved uniform stellar diameter of  $2.39 \pm 0.28$  mas is significantly better than the fit by a point-like source (SNR = 39.2 and 27.0 for the two cases, respectively). The relatively large error is mainly due to the slow time sampling, but the value is approximately consistent with the estimate of the angular diameter for this M0 giant which is 1.9 mas using the empirical calibration by van Belle (1999).

There are no previous direct determinations of the angular diameter of IRC + 20101 in the literature, and no observations by high angular resolution methods including no other LO observations.

### 4.4. SAO 77838

The data and best fit by a point-source for SAO 77838 are shown on the right side of Fig. 2. The SNR ratio for this data set is one of the highest obtained during commissioning, and we have used the method referenced in Sec. 3 to put an upper limit on the angular size of SAO 77838 of  $1.45 \pm 0.65$  mas. This can be satisfactorily compared with an empirical estimate of 1.1 mas for the angular diameter of this K7 giant, located at  $\approx 138$  pc, using the calibration by van Belle (1999). It reinforces the validity of using TIRCAM2 and

the LO method to measure angular diameters in the mas range.

As was the case for IRC + 20101, also for SAO 77838 there are no previous LO observations reported and no relevant literature entries with direct measurements.

## 5. Planned Developments and Outlook

Using those data from Table 1 for which a fit could be made, we plot in Fig. 4 the SNR as a function of the  $K$  magnitude. The scatter is significant, as expected given that LO events occur under a large range of sky background (strongly dependent in turn on the illumination fraction and the distance to the terminator) and other parameters. Nevertheless, a trend is clearly visible already in these preliminary commissioning data, with SAO 98770 being an outlier in virtue of the sampling and integration time being 4 times longer than for the rest. We can thus conclude that under the standard sub-array configuration ( $32 \times 32$  pixels at  $\sim 10$  ms) the fast photometry mode of TIRCAM2 can be sensitive to about  $K = 9$  mag, to detect the occultation of a single unresolved sources, i.e. with  $\text{SNR} \approx 1$ . As a rough guideline, the detection of 1:1 binary would require an  $\text{SNR} \gtrsim 3$ , while angular diameter determination would require an  $\text{SNR} \gtrsim 10$ , or  $K \lesssim 6$  mag.

This opens the possibility of using LO to investigate angular diameters and binaries with targets available essentially any night that the Moon is

up and the phase 2 days away from full Moon. To put this in context, we have used the 2MASS catalog truncated to the limit  $K \leq 8.5$  mag to compute occultations for the whole year of 2023 visible from the Devasthal site. Within acceptable limits of lunar phase and elevation, a total of 18,460 LO events would be observable in principle over the year, of which 8766 disappearances. As each LO event takes less than an half hour of telescope time (including overheads, initial settings, etc.), this program is ideal to fill the gaps in the telescope schedule and to utilize the less demanded bright moon period. However, due to non-availability of an automated observational sequencer at the telescope, this program demands availability of dedicated and trained manpower at the site. In order to efficiently conduct this LO program from the telescope, development of both the observing sequencer and data reduction pipeline is required.

The current main limitation is the sampling time, which at 10 ms is 2 or 3 times longer than optimal for LO events (see e.g. Richichi *et al.*, 1996). We have been considering solutions, at both the software and the hardware level. A software approach with the current FPA controller may be limited due to the limitations of the current TIRCAM2 hardware. A more promising approach would be the installation of a new faster commercial controller, or the in-house design of a new one. These possibilities are currently under exploration.

## 6. Conclusions

The TIRCAM2 instrument at the DOT 3.6-m telescope in Devasthal, northern India, is an Imager originally designed to cover the  $J$  to  $L$  near-infrared bands ( $\approx 1\text{--}4 \mu\text{m}$ ) with an InSb Aladdin  $512 \times 512$  detector. The minimum full frame read-out time is 256 ms. Having in mind the requirements for LO observations, we have developed a fast photometry mode which makes use of a  $32 \times 32$  sub-array with read-out time just under 10 ms.

This mode has been commissioned by observing 18 LO events, of which 12 were successful in recording the characteristic diffraction patterns. Among them, we could measure two stellar angular diameters and two binary stars. The rest of the data were consistent with unresolved point sources. The sensitivity is established to be close to  $K \sim 9$  mag. This in turn translates to several thousands of LO events observable in principle from the Devasthal site each year.

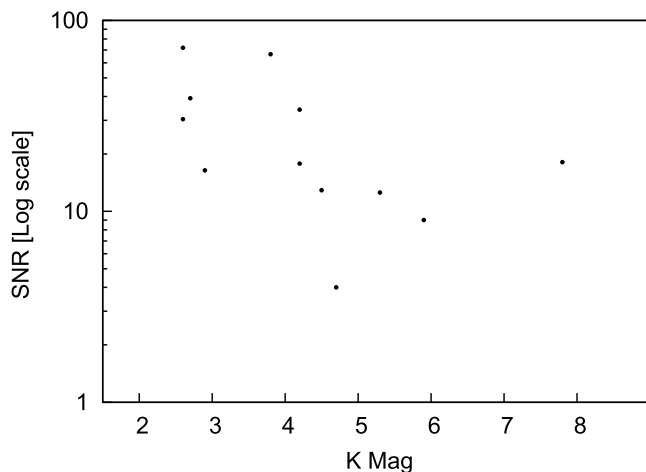


Fig. 4. Plot of the SNR of the LO best fit as a function of the  $K$  magnitude, using the applicable data from Table 1. The point close to  $K = 8$  mag (SAO 98770) stands out from the main trend because it was recorded at much slower rate than the rest. Discussions are given in the text.

The observation procedures and the data flow, resulting in 3D standard FITS cubes, have been thoroughly tested and the mode is now publicly offered to interested users. Improvements are being considered to bring the sampling time down to very few milliseconds.

## Acknowledgments

We dedicate this paper to the memory of the late Prof. Anil K. Pandey, who led the establishment of a LO program at ARIES. This work has made use of the SIMBAD data base, operated at CDS, Strasbourg, France. It is a pleasure to thank the technical team for the 3.6 m DOT, as well as the members of the IR astronomy group at TIFR, for their support during the observing runs. SS acknowledges the support of the Department of Science and Technology, Government of India, under Project No. DST/INT/Thai/P-15/2019. DKO and MBN acknowledge the support of the Department of Atomic Energy, Government of India, under Project Identification No. RTI 4002.

## References

- Baug, T., Ojha, D. K., Ghosh, S. K. *et al.* [2018] *J. Astron. Instrum.* **7**, 1850003.
- Chandrasekhar, T., Ashok, N. M. & Ragland, S. [1993] *Bull. Astron. Soc. India* **21**, 499.
- Chandrasekhar, T. & Baug, T. [2010] *MNRAS* **408**, 1006.
- Ghosh, S., Ojha, D. K., Sharma, S. *et al.* [2022] *J. Astrophys. Astron.* **43**, 16.
- Guerrero, C. A., Rosales-Ortega, F. F., Escobedo, G. *et al.* [2020] *MNRAS* **495**, 806.
- Horch, E. P., van Belle, G. T., Davidson, J. W. *et al.* [2015] *AJ* **150**, 151.
- Kumar, B., Omar, A., Maheswar, G. *et al.* [2018] *Bull. Soc. R. Sci. Liege* **87**, 29.
- Kumar, A., Pandey, S. B., Singh, A. *et al.* [2022] *J. Astrophys. Astron.* **43**, 27.
- Naik, M. B., Ojha, D. K., Ghosh, S. K. *et al.* [2012] *Bull. Soc. R. Sci. Liege* **40**, 531.
- Nather, R. E. & McCants, M. M. [1970] *AJ* **75**, 963.
- Ojha, D., Ghosh, S. K., Sharma, S. *et al.* [2018] *Bull. Soc. R. Sci. Liege* **87**, 58.
- Omar, A., Kumar, T. S., Krishna, R. B. *et al.* [2019] arXiv:1902.05857.
- Richichi, A. [1989] *A&A* **226**, 366.
- Richichi, A., Baffa, C., Calamai, G. *et al.* [1996] *AJ* **112**, 2786.
- Richichi, A., di Giacomo, A., Lisi, F. *et al.* [1992] *A&A* **265**, 535.
- Richichi, A., Dyachenko, V., Pandey, A. K. *et al.* [2017] *MNRAS* **464**, 231.
- Richichi, A., Fors, O., Cusano, F. *et al.* [2014] *AJ* **147**, 57.
- Richichi, A., Sharma, S., Sinha, T. *et al.* [2020] *MNRAS* **498**, 2263.
- Robbe-Dubois, S., Cruzalèbes, P., Berio, P. *et al.* [2022] *MNRAS* **510**, 82.
- Stalin, C. S., Sagar, R., Pant, P. *et al.* [2001] *Bull. Soc. R. Sci. Liege* **29**, 39.
- Tarasov, A. E. [2016] *Astron. Lett.* **42**, 598.
- Tej, A. & Chandrasekhar, T. [2000] *MNRAS* **317**, 687.
- van Belle, G. T. [1999] *Publ. Astron. Soc. Pac.* **111**, 1515.